Progress In Electromagnetics Research B, Vol. 63, 249–261, 2015

Dyadic Green's Functions for a Parallel Plate Waveguide Filled with Anisotropic Uniaxial Media

Neil G. Rogers* and Michael J. Havrilla

Abstract—The dyadic Green's functions for magnetic and electric currents immersed in a parallel plate waveguide (PPWG) filled with dielectric-magnetic anisotropic uniaxial media are developed via a field-based approach. First, the principal Green's function is derived from the forced wave equation for currents immersed in an unbounded uniaxial media. Next, the scattered Green's function is developed from the unforced wave equation. Finally, the total Green's function is found by superposition and subsequent application of the appropriate boundary conditions. The Green's functions are derived from Maxwell's equations, using a spectral domain analysis and reveals several key physical insights. First, the expected longitudinal depolarization dyads are observed. The expected depolarizing terms arise through careful application of complex-plane analysis, leading to expressions that are valid both internal and external to the source region. Secondly, the identification and decomposition of the total Green's function into TE^z and TM^z field contributions is demonstrated. Thirdly, the mathematical forms of the principal and total Green's functions are shown to be physically intuitive.

The primary contribution of this research is the development of the Green's functions for a parallel plate waveguide containing a dielectric and magnetic uniaxial medium directly from Maxwell's equations. Prior derivations considered dielectric-only uniaxial media in a parallel-plate waveguide, due to the relative ease of analysis and readily available inverse identities found in [7]. Inclusion of magnetic uniaxial characteristics adds considerable complexity (since no simplifying identities are available) and provides additional insight into the field behavior, thus representing a significant contribution to the electromagnetic analysis of complex media. Finally, practical applications of the Green's functions are considered, such as the non-destructive electromagnetic characterization of a variety of anisotropic uniaxial media.

1. INTRODUCTION

Electromagnetic characterization is the process of determining the constitutive parameters of a given material (permeability, permittivity and the magnetoelectric coupling parameters). Methods for obtaining these parameters have existed for many years [5, 6, 12, 18, 24, 26]. Notably, methods such as the two-Flanged Waveguide Measurement Technique (tFWMT) employed in [18, 19, 26] require a Green's function subject to the appropriate boundary conditions. Several methods exist for obtaining the Green's functions for this type of configuration, but the complexity of the solution is heavily dependent on the method and the type of media under consideration. For example, the well-known method of vector potentials has commonly been used in simple media (linear, homogeneous, isotropic) [3, 10, 15, 27], but becomes difficult to employ when dealing with anisotropic media. More recently, the technique of scalar potentials has been applied to obtain the Green's functions for both anisotropic and bianisotropic media[11, 14, 21–23, 25, 30, 31, 33–37]. In spite of the growing interest in

Received 14 June 2015, Accepted 28 September 2015, Scheduled 6 October 2015
* Corresponding author: Neil G. Rogers (neil.rogers@us.af.mil).
The authors are with the Department of Electrical and Computer Engineering, Air Force Institute of Technology, 2950 Hobson Way, WPAFB, OH 45433, USA.

complex media and the appearance of several forms of the principal Green's functions for uniaxial media, a field-based development of the total Green's functions for electric and magnetic currents immersed in a PPWG filled with dielectric magnetic uniaxial media has not appeared in previous literature. This article presents a detailed development of the PPWG Green's functions directly from Maxwell's equations, subject to the parallel plate boundary conditions, which are assumed to be perfect electrical conductors (PEC). For isotropic media, solving Maxwell's equations in a direct manner is a fairly straightforward task, but becomes significantly more complicated when considering anisotropic media. Most recently, in [16], Maxwell's equations are solved directly for a magnetic current immersed in a uniaxial, dielectric-filled PPWG structure. However, the more general case is solved here, incorporating the possibilities of both dielectric and magnetic anisotropy, with excitation by an electric and magnetic current. The total solution will be a superposition of the principal and reflected portion, subject to PEC boundary conditions in the longitudinal (z) direction. These expressions represents a significant contribution to the electromagnetic theory of anisotropic media.

After the Green's functions are developed, a physical interpretation will be provided. One benefit of the direct (referred to as field-based) solution to Maxwell's equation is the improved physical insight into the modal behavior that is gained. We will conclude with a brief discussion of a specific application of these expressions in the electromagnetic characterization of anisotropic media.

It will be helpful to clarify the nomenclature used in this article. The subscripts e and h are used to represent electric and magnetic components, respectively. When two components are combined, such as eh-type, we mean the electric field (e) maintained by a magnetic source (h).

2. ELECTRIC FIELD DYADIC GREEN'S FUNCTION

Consider a magnetic current, $\vec{J}_h$, and an electric current, $\vec{J}_e$, immersed in a PPWG structure filled with uniaxially dielectric and magnetic media having permittivity $\overleftrightarrow{\varepsilon} = \hat{\mathbf{x}}\varepsilon_t\hat{\mathbf{x}} + \hat{\mathbf{y}}\varepsilon_t\hat{\mathbf{y}} + \hat{\mathbf{z}}\varepsilon_z\hat{\mathbf{z}}$ and permeability $\overleftrightarrow{\mu} = \hat{\mathbf{x}}\mu_t\hat{\mathbf{x}} + \hat{\mathbf{y}}\mu_t\hat{\mathbf{y}} + \hat{\mathbf{z}}\mu_z\hat{\mathbf{z}}$, as depicted in Figure 1. The total fields in this environment comprise a principal (i.e., forced) wave contribution and a reflected (i.e., unforced) wave contribution. Maxwell's curl equations for the principal and reflected contributions are, respectively,

$$\begin{aligned} \overleftrightarrow{\nabla} \cdot \vec{E}^p(\vec{\rho}, z) &= -\vec{J}_h(\vec{\rho}, z) - j\omega\overleftrightarrow{\mu}\cdot\vec{H}^p(\vec{\rho}, z) \\ \overleftrightarrow{\nabla} \cdot \vec{H}^p(\vec{\rho}, z) &= \vec{J}_e(\vec{\rho}, z) + j\omega\overleftrightarrow{\varepsilon}\cdot\vec{E}^p(\vec{\rho}, z) \end{aligned} \tag{1}$$

$$\begin{aligned} \overleftrightarrow{\nabla} \cdot \vec{E}^r(\vec{\rho}, z) &= -j\omega\overleftrightarrow{\mu}\cdot\vec{H}^r(\vec{\rho}, z) \\ \overleftrightarrow{\nabla} \cdot \vec{H}^r(\vec{\rho}, z) &= j\omega\overleftrightarrow{\varepsilon}\cdot\vec{E}^r(\vec{\rho}, z) \end{aligned} \tag{2}$$

where $\overleftrightarrow{\nabla} = \nabla \times \overleftrightarrow{I} = \overleftrightarrow{I} \times \nabla$, $\nabla = \hat{\mathbf{x}}\frac{\partial}{\partial x} + \hat{\mathbf{y}}\frac{\partial}{\partial y} + \hat{\mathbf{z}}\frac{\partial}{\partial z}$ and $\vec{\rho} = \hat{\mathbf{x}}x + \hat{\mathbf{y}}y$.

2.1. Principal (Forced) Solution

Since the principal solution is assumed to exist in unbounded space, we are prompted to apply a Fourier transform. Given the uniaxial nature of the media, we transform separately in the transverse and

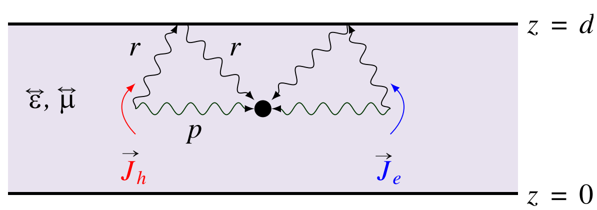

Figure 1. A PPWG filled with uniaxial media, where the distinguished (z) axis is normal to the PEC walls and the parallel plates are assumed to be infinite in the x-y plane. The principal (p) and reflected (r) waves are drawn to illustrate the superposition principle used in determining the total solution.

longitudinal dimensions. Therefore, using the generic transform pairs

$$\tilde{f}(\vec{\lambda}_\rho, z) = \iint_{-\infty}^{\infty} f(\vec{\rho}, z) e^{-j\vec{\lambda}_\rho \cdot \vec{\rho}} dx dy, \quad f(\vec{\rho}, z) = \frac{1}{(2\pi)^2} \iint_{-\infty}^{\infty} \tilde{f}(\vec{\lambda}_\rho, z) e^{j\vec{\lambda}_\rho \cdot \vec{\rho}} d\lambda_x d\lambda_y \tag{3}$$

and

$$\tilde{\tilde{f}}(\vec{\lambda}_\rho, \lambda_z) = \int_{-\infty}^{\infty} \tilde{f}(\vec{\lambda}_\rho, z) e^{-j\lambda_z z} dz, \quad \tilde{f}(\vec{\lambda}_\rho, z) = \frac{1}{2\pi} \int_{-\infty}^{\infty} \tilde{\tilde{f}}(\vec{\lambda}_\rho, \lambda_z) e^{j\lambda_z z} d\lambda_z \tag{4}$$

we are able to write the principal curl equations as

$$j\overleftrightarrow{\lambda} \cdot \tilde{\tilde{\vec{E}}}^p(\vec{\lambda}_\rho, z) = -\tilde{\tilde{\vec{J}}}_h(\vec{\lambda}_\rho, \lambda_z) - j\omega\overleftrightarrow{\mu} \cdot \tilde{\tilde{\vec{H}}}^p(\vec{\lambda}_\rho, z) \tag{5}$$

$$j\overleftrightarrow{\lambda} \cdot \tilde{\tilde{\vec{H}}}^p(\vec{\lambda}_\rho, z) = \tilde{\tilde{\vec{J}}}_e(\vec{\lambda}_\rho, \lambda_z) + j\omega\overleftrightarrow{\varepsilon} \cdot \tilde{\tilde{\vec{E}}}^p(\vec{\lambda}_\rho, z) \tag{6}$$

with $\overleftrightarrow{\lambda} = \overleftrightarrow{I} \times \vec{\lambda} = \vec{\lambda} \times \overleftrightarrow{I}$ and $\vec{\lambda}_\rho = \hat{\mathbf{x}}\lambda_x + \hat{\mathbf{y}}\lambda_y$. It is observed that the coupled system of equations can be solved by the usual matrix methods, leading to

$$\tilde{\tilde{\vec{E}}}^p = -j\omega\overleftrightarrow{w}_e^{-1} \cdot \overleftrightarrow{\mu} \cdot \tilde{\tilde{\vec{J}}}_e - j\overleftrightarrow{w}_e^{-1} \cdot \overleftrightarrow{\mu} \cdot \overleftrightarrow{\lambda} \cdot \overleftrightarrow{\mu}^{-1} \cdot \tilde{\tilde{\vec{J}}}_h = \tilde{\tilde{\overleftrightarrow{G}}}{}^p_{ee} \cdot \tilde{\tilde{\vec{J}}}_e + \tilde{\tilde{\overleftrightarrow{G}}}{}^p_{eh} \cdot \tilde{\tilde{\vec{J}}}_h \tag{7}$$

$$\tilde{\tilde{\vec{H}}}^p = j\overleftrightarrow{w}_h^{-1} \cdot \overleftrightarrow{\varepsilon} \cdot \overleftrightarrow{\lambda} \cdot \overleftrightarrow{\varepsilon}^{-1} \cdot \tilde{\tilde{\vec{J}}}_e - j\omega\overleftrightarrow{w}_h^{-1} \cdot \overleftrightarrow{\varepsilon} \cdot \tilde{\tilde{\vec{J}}}_h = \tilde{\tilde{\overleftrightarrow{G}}}{}^p_{he} \cdot \tilde{\tilde{\vec{J}}}_e + \tilde{\tilde{\overleftrightarrow{G}}}{}^p_{hh} \cdot \tilde{\tilde{\vec{J}}}_h \tag{8}$$

where $\overleftrightarrow{w}_e = -\overleftrightarrow{\mu} \cdot \overleftrightarrow{\lambda} \cdot \overleftrightarrow{\mu}^{-1} \cdot \overleftrightarrow{\lambda} - \overleftrightarrow{k}^2$, $\overleftrightarrow{w}_h = -\overleftrightarrow{\varepsilon} \cdot \overleftrightarrow{\lambda} \cdot \overleftrightarrow{\varepsilon}^{-1} \cdot \overleftrightarrow{\lambda} - \overleftrightarrow{k}^2$. Note that, due to the diagonal form of $\overleftrightarrow{\varepsilon}$ and $\overleftrightarrow{\mu}$, we have $\overleftrightarrow{k}^2 = \omega^2\overleftrightarrow{\varepsilon} \cdot \overleftrightarrow{\mu} = \omega^2\overleftrightarrow{\mu} \cdot \overleftrightarrow{\varepsilon}$.

Although we have now determined expressions for the spectral domain Green's functions, a considerable amount of algebraic effort is required to determine $\overleftrightarrow{w}_e^{-1}$ and $\overleftrightarrow{w}_h^{-1}$. In [16], only one of the constitutive dyads is considered to be anisotropic. Therefore, finding $\overleftrightarrow{w}_e^{-1}$ and $\overleftrightarrow{w}_h^{-1}$ is considerably simplified by utilizing a dyadic identity found in equation 1.128 of [7]. In this work, given the additional vector terms in the dyads $\overleftrightarrow{w}_e$ and $\overleftrightarrow{w}_h$, such a simplification is not possible, because no corresponding inverse identity exists. Not only does this increase the algebraic effort in computing the inverse dyads, it also requires the Green's functions to be calculated on a component-by-component basis. For the sake of brevity, we will only detail the development of $\overleftrightarrow{w}_e^{-1}$, as $\overleftrightarrow{w}_h^{-1}$ can be found by similar methods (and also by duality). Using the definition of $\overleftrightarrow{\lambda}$, namely

$$\overleftrightarrow{\lambda} = \overleftrightarrow{I} \times \vec{\lambda} = (\hat{\mathbf{x}}\hat{\mathbf{x}} + \hat{\mathbf{y}}\hat{\mathbf{y}} + \hat{\mathbf{z}}\hat{\mathbf{z}}) \times (\hat{\mathbf{x}}\lambda_x + \hat{\mathbf{y}}\lambda_y + \hat{\mathbf{z}}\lambda_z) = \begin{bmatrix} 0 & -\lambda_z & \lambda_y \\ \lambda_z & 0 & -\lambda_x \\ -\lambda_y & \lambda_x & 0 \end{bmatrix}, \tag{9}$$

straightforward mathematical manipulation leads to the following result:

$$\overleftrightarrow{w}_e = -\overleftrightarrow{\mu} \cdot \overleftrightarrow{\lambda} \cdot \overleftrightarrow{\mu}^{-1} \cdot \overleftrightarrow{\lambda} - \overleftrightarrow{k}^2 = \begin{bmatrix} \lambda_z^2 - k_\rho{}^2 + \frac{\mu_t}{\mu_z}\lambda_y^2 & -\frac{\mu_t}{\mu_z}\lambda_x\lambda_y & -\lambda_x\lambda_z \\ -\frac{\mu_t}{\mu_z}\lambda_x\lambda_y & \lambda_z^2 - k_\rho{}^2 + \frac{\mu_t}{\mu_z}\lambda_x{}^2 & -\lambda_y\lambda_z \\ -\frac{\mu_z}{\mu_t}\lambda_x\lambda_z & -\frac{\mu_z}{\mu_t}\lambda_y\lambda_z & \frac{\mu_z}{\mu_t}\lambda_\rho^2 - k_z^2 \end{bmatrix} \tag{10}$$

with $k_\rho^2 = \omega^2\varepsilon_t\mu_t$ and $k_z^2 = \omega^2\varepsilon_z\mu_z$. The inverse may now be computed by the adjoint method, whereby

$$\overleftrightarrow{A}^{-1} = \frac{\mathrm{adj}(\overleftrightarrow{A})}{\det(\overleftrightarrow{A})} \tag{11}$$

Defining the eigenvalues $\lambda_{z\psi}^2 = k_\rho^2 - \frac{\mu_t}{\mu_z}\lambda_\rho^2$ and $\lambda_{z\theta}^2 = k_\rho^2 - \frac{\varepsilon_t}{\varepsilon_z}\lambda_\rho^2$, we are able to find the determinant of $\overleftrightarrow{w}_e$ as

$$\det(\overleftrightarrow{w}_e) = -k_z^2\left(\lambda_z^2 - \lambda_{z\theta}^2\right)\left(\lambda_z^2 - \lambda_{z\psi}^2\right) \tag{12}$$

The adjoint is computed by the co-factor matrix adj $(\overleftrightarrow{w}_e) = \overleftrightarrow{C}^T$, $C_{mn} = (-1)^{m+n} M_{mn}$, where M_{mn} is the determinant of the minor with the mth row and nth column removed. Utilizing this definition and a considerable amount of mathematical manipulation, we find (where the indices of the M matrix have **not** been rearranged, in order to clearly show the transpose operation):

$$
\begin{aligned}
\text{adj}\,(\overleftrightarrow{w}_e) &= \overleftrightarrow{C}^T = \begin{bmatrix} M_{11} & -M_{21} & M_{31} \\ -M_{12} & M_{22} & -M_{32} \\ M_{13} & -M_{23} & M_{33} \end{bmatrix} \\
M_{11} &= \left(\lambda_z^2 - \lambda_{z\theta}^2\right)\left(-\frac{\varepsilon_z\mu_z}{\varepsilon_t\mu_t}\lambda_{z\psi}^2\right) - \frac{\varepsilon_z}{\varepsilon_t}\lambda_y^2\left(\frac{\varepsilon_t\mu_z}{\varepsilon_z\mu_t}\lambda_z^2 - \lambda_{z\psi}^2\right) \\
M_{21} &= -\frac{\varepsilon_z}{\varepsilon_t}\lambda_x\lambda_y\left(\frac{\varepsilon_t\mu_z}{\varepsilon_z\mu_t}\lambda_z^2 - \lambda_{z\psi}^2\right) \\
M_{31} &= \lambda_x\lambda_z\left(\lambda_z^2 - \lambda_{z\theta}^2\right) \\
M_{12} &= -\frac{\varepsilon_z}{\varepsilon_t}\lambda_x\lambda_y\left(\frac{\varepsilon_t\mu_z}{\varepsilon_z\mu_t}\lambda_z^2 - \lambda_{z\psi}^2\right) \\
M_{22} &= \left(\lambda_z^2 - \lambda_{z\theta}^2\right)\left(-\frac{\varepsilon_z\mu_z}{\varepsilon_t\mu_t}\lambda_{z\psi}^2\right) - \frac{\varepsilon_z}{\varepsilon_t}{\lambda_x}^2\left(\frac{\varepsilon_t\mu_z}{\varepsilon_z\mu_t}\lambda_z^2 - \lambda_{z\psi}^2\right) \\
M_{32} &= \left(-\lambda_y\lambda_z\right)\left(\lambda_z^2 - \lambda_{z\theta}^2\right) \\
M_{13} &= \left(\lambda_z^2 - \lambda_{z\theta}^2\right)\left(\frac{\mu_z}{\mu_t}\lambda_x\lambda_z\right) \\
M_{23} &= \left(\lambda_z^2 - \lambda_{z\theta}^2\right)\left(-\frac{\mu_z}{\mu_t}\lambda_y\lambda_z\right) \\
M_{33} &= \left(\lambda_z^2 - k_\rho^2\right)\left(\lambda_z^2 - \lambda_{z\theta}^2\right)
\end{aligned}
\tag{13}
$$

Now, recalling the definition of the eh-type Green's function from (7) and simplifying as necessary, we have the spectral domain Green's function as

$$
\begin{aligned}
\overleftrightarrow{\tilde{\tilde{G}}}{}^p_{eh} &= -j\overleftrightarrow{w}_e^{-1}\cdot\overleftrightarrow{\mu}\cdot\overleftrightarrow{\lambda}\cdot\overleftrightarrow{\mu}^{-1} = \begin{bmatrix} \tilde{\tilde{G}}^p_{eh,xx} & \tilde{\tilde{G}}^p_{eh,xy} & \tilde{\tilde{G}}^p_{eh,xz} \\ \tilde{\tilde{G}}^p_{eh,yx} & \tilde{\tilde{G}}^p_{eh,yy} & \tilde{\tilde{G}}^p_{eh,yz} \\ \tilde{\tilde{G}}^p_{eh,zx} & \tilde{\tilde{G}}^p_{eh,zy} & \tilde{\tilde{G}}^p_{eh,zz} \end{bmatrix} \\
&= j\frac{\begin{bmatrix} -\lambda_z M_{21} - \dfrac{\lambda_y\mu_z}{\mu_t}M_{31} & \dfrac{\lambda_x\mu_z}{\mu_t}M_{31} - \lambda_z M_{11} & \dfrac{\lambda_y\mu_t}{\mu_z}M_{11} + \dfrac{\lambda_x\mu_t}{\mu_z}M_{21} \\ \lambda_z M_{22} + \dfrac{\lambda_y\mu_z}{\mu_t}M_{32} & \lambda_z M_{12} - \dfrac{\lambda_x\mu_z}{\mu_t}M_{32} & -\dfrac{\lambda_y\mu_t}{\mu_z}M_{12} - \dfrac{\lambda_x\mu_t}{\mu_z}M_{22} \\ -\lambda_z M_{23} - \dfrac{\lambda_y\mu_z}{\mu_t}M_{33} & \dfrac{\lambda_x\mu_z}{\mu_t}M_{33} - \lambda_z M_{13} & \dfrac{\lambda_y\mu_t}{\mu_z}M_{13} + \dfrac{\lambda_x\mu_t}{\mu_z}M_{23} \end{bmatrix}}{-k_z^2\left(\lambda_z^2 - \lambda_{z\theta}^2\right)\left(\lambda_z^2 - \lambda_{z\psi}^2\right)}
\end{aligned}
\tag{14}
$$

Using (4), we perform the inverse Fourier transformation on the λ_z variable to find the $(\vec{\lambda}_\rho, z)$ domain Green's function representation of the electric field maintained by a generic magnetic current existing between $z = 0$ and $z = d$:

$$
\vec{\tilde{E}}{}^p_h(\vec{\lambda}_\rho, z) = \int_0^d \overleftrightarrow{\tilde{G}}{}^p_{eh}(\vec{\lambda}_\rho; z - z')\cdot\vec{\tilde{J}}_h(\vec{\lambda}_\rho, z')dz' \tag{15}
$$

where

$$
\overleftrightarrow{\tilde{G}}{}^p_{eh}(\vec{\lambda}_\rho; z - z') = \frac{1}{2\pi}\int_{-\infty}^{\infty} \overleftrightarrow{\tilde{\tilde{G}}}{}^p_{eh}(\vec{\lambda}_\rho, \lambda_z)e^{j\lambda_z(z-z')}d\lambda_z \tag{16}
$$

The $(\vec{\lambda}_\rho, z)$ domain Green's function can be determined by complex plane analysis. Specifically, we apply Cauchy's Integral Theorem, Jordan's Lemma and Cauchy's Integral Formula to each element of (16). As in [16], the Green's function is found to be a superposition of a TE^z and TM^z contribution.

$$\begin{aligned}
\overleftrightarrow{\tilde{G}}{}^p_{eh}(\vec{\lambda}_\rho|z-z') &= \begin{bmatrix} \tilde{G}^p_{eh,xx} & \tilde{G}^p_{eh,xy} & \tilde{G}^p_{eh,xz} \\ \tilde{G}^p_{eh,yx} & \tilde{G}^p_{eh,yy} & \tilde{G}^p_{eh,yz} \\ \tilde{G}^p_{eh,zx} & \tilde{G}^p_{eh,zy} & \tilde{G}^p_{eh,zz} \end{bmatrix} = \overleftrightarrow{\tilde{G}}{}^{p,\mathrm{TE}}_{eh} + \overleftrightarrow{\tilde{G}}{}^{p,\mathrm{TM}}_{eh} \\
\tilde{G}^p_{eh,xx} &= -\mathrm{sgn}(z-z')\frac{\lambda_x\lambda_y}{2\lambda_\rho^2}e^{-j\lambda_{z\theta}|z-z'|} + \mathrm{sgn}(z-z')\frac{\lambda_x\lambda_y}{2\lambda_\rho^2}e^{-j\lambda_{z\psi}|z-z'|} \\
\tilde{G}^p_{eh,xy} &= -\mathrm{sgn}(z-z')\frac{\lambda_y^2}{2\lambda_\rho^2}e^{-j\lambda_{z\theta}|z-z'|} - \mathrm{sgn}(z-z')\frac{\lambda_x^2}{2\lambda_\rho^2}e^{-j\lambda_{z\psi}|z-z'|} \\
\tilde{G}^p_{eh,xz} &= -\frac{\frac{\mu_t}{\mu_z}\lambda_y}{2\lambda_{z\theta}}e^{-j\lambda_{z\theta}|z-z'|} - 0 \\
\tilde{G}^p_{eh,yx} &= \mathrm{sgn}(z-z')\frac{\lambda_x^2}{2\lambda_\rho^2}e^{-j\lambda_{z\theta}|z-z'|} + \mathrm{sgn}(z-z')\frac{\lambda_y^2}{2\lambda_\rho^2}e^{-j\lambda_{z\psi}|z-z'|} \qquad (17) \\
\tilde{G}^p_{eh,yy} &= \mathrm{sgn}(z-z')\frac{\lambda_x\lambda_y}{2\lambda_\rho^2}e^{-j\lambda_{z\theta}|z-z'|} - \mathrm{sgn}(z-z')\frac{\lambda_x\lambda_y}{2\lambda_\rho^2}e^{-j\lambda_{z\psi}|z-z'|} \\
\tilde{G}^p_{eh,yz} &= \frac{\frac{\mu_t}{\mu_z}\lambda_x}{2\lambda_{z\theta}}e^{-j\lambda_{z\theta}|z-z'|} + 0 \\
\tilde{G}^p_{eh,zx} &= 0 + \frac{\frac{\varepsilon_t}{\varepsilon_z}\lambda_y}{2\lambda_{z\psi}}e^{-j\lambda_{z\psi}|z-z'|} \\
\tilde{G}^p_{eh,zy} &= 0 - \frac{\frac{\varepsilon_t}{\varepsilon_z}\lambda_x}{2\lambda_{z\psi}}e^{-j\lambda_{z\psi}|z-z'|} \\
\tilde{G}^p_{eh,zz} &= 0 + 0
\end{aligned}$$

Although we have only given the results here for the eh-type Green's function, an analogous process will produce the ee-type Green's function. There is, however, one point of difference where care must be taken in the application of Cauchy's integral theorem. Namely, Jordan's Lemma requires $\lim_{\lambda_z\to\infty} \overleftrightarrow{\tilde{\tilde{G}}}{}^p = 0$ in order to properly apply Cauchy's Integral Theorem. This is found to be true for all components of the eh-type Green's function and the ee-type Green's function **except** $\tilde{\tilde{G}}^p_{ee,zz}$. In this case, we find:

$$\lim_{\lambda_z\to\infty} \tilde{\tilde{G}}^p_{zz,ee} = -\frac{1}{j\omega\varepsilon_z}$$

Therefore, in order to ensure Jordan's Lemma is satisfied, we add and subtract this term to the $\hat{\mathbf{z}}\hat{\mathbf{z}}$ component before performing the complex plane integration. When transforming from the $(\vec{\lambda}_\rho, \lambda_z)$ domain to the $(\vec{\lambda}_\rho, z)$ domain, this leads to the well-known longitudinal depolarizing term (using the properties of the Dirac delta function). A similar term is found when computing the hh-type Green's function. These terms are the longitudinal depolarizing terms reported in many previous works [1, 2, 4, 8, 9, 13, 17, 20, 28, 29, 32, 38]. Physically, these depolarizing terms account for the source point singularity and ensure the expressions are valid for the entire region under consideration, both internal and external to the source. Notably, the same term is derived in [16] through an application of Leibnitz's rule to Faraday's law in the $(\vec{\lambda}_\rho, z)$ domain. Both methods produce equivalent results. Additionally, this term is found when using a scalar potential method [17] to find the principal Green's function.

One final point of interest is, upon expanding the expressions given in [16] (which are given for a dielectric-only uniaxial material) and comparing term-by-term with the expressions above, we are able to find a vectorized form for the more general media. However, it is not clear to the authors how such a form would be developed from the coupled solutions to Maxwell's equations given in (1). The vectorized forms given here are again found to be combinations of TE^z and TM^z contributions. However, they are not used in any further computations, since they do not arise from a rigorous mathematical development. They are presented merely to demonstrate the similarities between a dielectric-only uniaxial material and a dielectric and magnetic uniaxial material.

$$\begin{aligned}\tilde{\overleftrightarrow{G}}{}^{p}_{eh}(\vec{\lambda}_\rho|z-z') \;=\;& \frac{\left(\hat{\lambda}_\rho\times\hat{\mathbf{z}}\right)\left(\hat{\lambda}_\rho\times\hat{\mathbf{z}}\right)\cdot\overleftrightarrow{\lambda}{}^{h}_{\theta}}{-2\lambda_{z\theta}}e^{-j\lambda_{z\theta}|z-z'|}\\ &+\frac{\overleftrightarrow{\lambda}{}^{h}_{\psi}-\left(1-\frac{\varepsilon_t\mu_z}{\varepsilon_z\mu_t}\right)\hat{\mathbf{z}}\hat{\mathbf{z}}\cdot\overleftrightarrow{\lambda}{}^{h}_{\psi}-\left(\hat{\lambda}_\rho\times\hat{\mathbf{z}}\right)\left(\hat{\lambda}_\rho\times\hat{\mathbf{z}}\right)\cdot\overleftrightarrow{\lambda}{}^{h}_{\psi}}{-2\lambda_{z\psi}}e^{-j\lambda_{z\psi}|z-z'|}\end{aligned} \tag{18}$$

where

$$\overleftrightarrow{\lambda}{}^{h}_{\alpha}=\hat{\mathbf{x}}\mathrm{sgn}(z-z')\lambda_{z\alpha}\hat{\mathbf{y}}+\hat{\mathbf{x}}\frac{\mu_t}{\mu_z}\lambda_y\hat{\mathbf{z}}-\hat{\mathbf{y}}\mathrm{sgn}(z-z')\lambda_{z\alpha}\hat{\mathbf{x}}-\hat{\mathbf{y}}\frac{\mu_t}{\mu_z}\lambda_x\hat{\mathbf{z}}-\frac{\mu_t}{\mu_z}\hat{\mathbf{z}}\lambda_y\hat{\mathbf{x}}+\frac{\mu_t}{\mu_z}\hat{\mathbf{z}}\lambda_x\hat{\mathbf{y}}\ldots\alpha=\theta,\psi \tag{19}$$

2.2. Reflected (Unforced) Solution

Now that we have determined the principal solution to the fields for unbounded media, we look for the scattered (reflected) solution in a source-free region bounded by parallel PEC plates. In this case, the plates are assumed to be unbounded in the x and y directions, leading to Fourier transforms in the transverse dimensions. Using a similar method as with the principal solution and intuition gained from that development, we can write the spectral domain versions of Maxwell's equations in a source-free region:

$$j\overleftrightarrow{\lambda}\cdot\tilde{\vec{E}}^{r}(\vec{\lambda}_\rho,\lambda_z) \;=\; -j\omega\overleftrightarrow{\mu}\cdot\tilde{\vec{H}}^{r}(\vec{\lambda}_\rho,\lambda_z) \tag{20}$$

$$j\overleftrightarrow{\lambda}\cdot\tilde{\vec{H}}^{r}(\vec{\lambda}_\rho,\lambda_z) \;=\; j\omega\overleftrightarrow{\varepsilon}\cdot\tilde{\vec{E}}^{r}(\vec{\lambda}_\rho,\lambda_z) \tag{21}$$

which can then be solved in a similar method as before, leading to an expression for the electric field:

$$\overleftrightarrow{w}_e\cdot\tilde{\vec{E}}^{r}=0 \tag{22}$$

Assuming the usual solution for forward and reverse traveling waves

$$\tilde{\vec{E}}^{r}(\lambda_\rho,z)=\tilde{\vec{E}}^{r\pm}_{o}(\lambda_\rho)e^{\mp j\lambda_z z}=\tilde{\vec{E}}^{r+}_{o}(\lambda_\rho)e^{-j\lambda_z z}+\tilde{\vec{E}}^{r-}_{o}(\lambda_\rho)e^{j\lambda_z z} \tag{23}$$

where the forward and reverse traveling electric field vectors are specified by the condensed notation† $\tilde{\vec{E}}^{r\pm}_{o}=\hat{\mathbf{x}}\tilde{\vec{E}}^{r\pm}_{ox}+\hat{\mathbf{y}}\tilde{\vec{E}}^{r\pm}_{oy}+\hat{\mathbf{z}}\tilde{\vec{E}}^{r\pm}_{oz}$. Now, a general solution to (22) is given by the eigenvalues:

$$\lambda_z=\pm\lambda_{z\theta},\pm\lambda_{z\psi} \tag{24}$$

These four solutions for λ_z represent the upward and downward propagating TE^z and TM^z waves. Decomposing the assumed solution into the orthogonal modes in the $(\vec{\lambda}_\rho,z)$ domain leads to

$$\begin{aligned}\tilde{\vec{E}}^{r}\left(\vec{\lambda}_\rho,z\right) \;=\;& \tilde{\vec{E}}^{r\theta}+\tilde{\vec{E}}^{r\psi}=\tilde{\vec{E}}^{r\theta+}_{o}\left(\vec{\lambda}_\rho\right)e^{-j\lambda_{z\theta}z}+\tilde{\vec{E}}^{r\theta-}_{o}\left(\vec{\lambda}_\rho\right)e^{j\lambda_{z\theta}z}\\ &+\tilde{\vec{E}}^{r\psi+}_{o}\left(\vec{\lambda}_\rho\right)e^{-j\lambda_{z\psi}z}+\tilde{\vec{E}}^{r\psi-}_{o}\left(\vec{\lambda}_\rho\right)e^{j\lambda_{z\psi}z}\end{aligned} \tag{25}$$

According to the superposition principle, we can examine the TE^z and TM^z contributions separately. Using a compact notation for the forward and reverse traveling TE^z and TM^z waves, (22) becomes

$$\overleftrightarrow{w}{}^{\theta}_{e}\cdot\tilde{\vec{E}}^{r\theta\pm}_{o}\left(\vec{\lambda}_\rho\right)e^{\mp j\lambda_{z\theta}z} \;=\; 0 \;\Longrightarrow\; \overleftrightarrow{w}{}^{\theta}_{e}\cdot\tilde{\vec{E}}^{r\theta\pm}_{o}=0 \tag{26}$$

$$\overleftrightarrow{w}{}^{\psi}_{e}\cdot\tilde{\vec{E}}^{r\psi\pm}_{o}\left(\vec{\lambda}_\rho\right)e^{\mp j\lambda_{z\psi}z} \;=\; 0 \;\Longrightarrow\; \overleftrightarrow{w}{}^{\psi}_{e}\cdot\tilde{\vec{E}}^{r\psi\pm}_{o}=0 \tag{27}$$

† A plus sign in the superscript represents a forward traveling wave, which corresponds to a *negative* exponential, due to the chosen time convention. The converse is true for reverse traveling waves.

Noting that $\vec{\tilde{E}}_o^{r\theta\pm} = \hat{\mathbf{x}}\tilde{E}_{ox}^{r\theta\pm} + \hat{\mathbf{y}}\tilde{E}_{oy}^{r\theta\pm} + \hat{\mathbf{z}}\tilde{E}_{oz}^{r\theta\pm}$ and $\vec{\tilde{E}}_o^{r\psi\pm} = \hat{\mathbf{x}}\tilde{E}_{ox}^{r\psi\pm} + \hat{\mathbf{y}}\tilde{E}_{oy}^{r\psi\pm} + \hat{\mathbf{z}}\tilde{E}_{oz}^{r\psi\pm}$, and after some algebraic effort, we are able to find:

$$\vec{\tilde{E}}^{r,\text{TE}} = \left(\hat{\mathbf{x}} - \hat{\mathbf{y}}\frac{\lambda_x}{\lambda_y}\right)\tilde{E}_{ox}^{r\theta\pm}e^{\mp j\lambda_{z\theta}z} \tag{28}$$

$$\vec{\tilde{E}}^{r,\text{TM}} = \left(\hat{\mathbf{x}}\tilde{E}_{ox}^{r\psi\pm} + \hat{\mathbf{y}}\frac{\lambda_y}{\lambda_x}\tilde{E}_{ox}^{r\psi\pm} \pm \hat{\mathbf{z}}\frac{\frac{\varepsilon_t}{\varepsilon_z}\lambda_\rho^2}{\lambda_x\lambda_{z\psi}}\tilde{E}_{ox}^{r\psi\pm}\right)e^{\mp j\lambda_{z\psi}z} \tag{29}$$

We note that these expressions are consistent with Gauss' law for a source-free region, providing confirmation regarding the form of the expressions. Here, we see there are four unknown scattering coefficients $(\tilde{E}_{ox}^{r\theta\pm}, \tilde{E}_{ox}^{r\psi\pm})$, which can be found by subsequent boundary condition enforcement. Furthermore, it can be easily shown that the decomposition of the electric field into orthogonal modes is justified, as $\vec{\tilde{E}}^{r,\text{TE}} \cdot \vec{\tilde{E}}^{r,\text{TM}} = 0$.

Now, the usual PEC boundary conditions are enforced on the total fields (the superposition of the principal and reflected solutions):

$$\tilde{E}_{ox}^{\theta}(z=0)=0, \quad \tilde{E}_{ox}^{\theta}(z=d)=0, \quad \tilde{E}_{ox}^{\psi}(z=0)=0, \quad \tilde{E}_{ox}^{\psi}(z=d)=0 \tag{30}$$

Upon enforcement of these boundary conditions, it is found that

$$\vec{\tilde{E}}_h^r(\vec{\lambda}_\rho, z) = \int_0^d \overleftrightarrow{\tilde{G}}_{eh}^r(\vec{\lambda}_\rho; z-z') \cdot \vec{\tilde{J}}_h(\vec{\lambda}_\rho, z')dz' \tag{31}$$

where

$$\overleftrightarrow{\tilde{G}}_{eh}^r(\vec{\lambda}_\rho; z-z') = \begin{bmatrix} \tilde{G}_{eh,xx}^{r,\text{TE}} & \tilde{G}_{eh,xy}^{r,\text{TE}} & \tilde{G}_{eh,xz}^{r,\text{TE}} \\ \tilde{G}_{eh,yx}^{r,\text{TE}} & \tilde{G}_{eh,yy}^{r,\text{TE}} & \tilde{G}_{eh,yz}^{r,\text{TE}} \\ 0 & 0 & 0 \end{bmatrix} + \begin{bmatrix} \tilde{G}_{eh,xx}^{r,\text{TM}} & \tilde{G}_{eh,xy}^{r,\text{TM}} & 0 \\ \tilde{G}_{eh,yx}^{r,\text{TM}} & \tilde{G}_{eh,yy}^{r,\text{TM}} & 0 \\ \tilde{G}_{eh,zx}^{r,\text{TM}} & \tilde{G}_{eh,zy}^{r,\text{TM}} & 0 \end{bmatrix} \tag{32}$$

The components can be written in the form:

$$\begin{aligned}\tilde{G}_{eh,y\alpha}^{r,\text{TE}} &= -\frac{\lambda_y}{\lambda_x}\tilde{G}_{eh,x\alpha}^{r,\text{TE}} \ldots \alpha = \lambda_x, \lambda_y \\ &= \left(-\frac{\lambda_y}{\lambda_x}\right)\left\{\frac{\alpha\lambda_y\lambda_{z\theta}\left[e^{-j\lambda_{z\theta}(z+z')} + e^{-j\lambda_{z\theta}(2d+z-z')} - e^{-j\lambda_{z\theta}(2d-z-z')} - e^{-j\lambda_{z\theta}(2d-z+z')}\right]}{-2\lambda_{z\theta}\lambda_\rho^2\left(1-e^{-j2\lambda_{z\theta}d}\right)}\right\}\end{aligned} \tag{33}$$

$$\begin{aligned}\tilde{G}_{eh,yz}^{r,\text{TE}} &= -\frac{\lambda_y}{\lambda_x}\tilde{G}_{eh,xz}^{r,\text{TE}} \\ &= \left(-\frac{\lambda_y}{\lambda_x}\right)\left\{\frac{\frac{\mu_t}{\mu_z}\lambda_y\lambda_\rho^2\left[-e^{-j\lambda_{z\theta}(z+z')} + e^{-j\lambda_{z\theta}(2d+z-z')} - e^{-j\lambda_{z\theta}(2d-z-z')} + e^{-j\lambda_{z\theta}(2d-z+z')}\right]}{-2\lambda_{z\theta}\lambda_\rho^2\left(1-e^{-j2\lambda_{z\theta}d}\right)}\right\}\end{aligned} \tag{34}$$

Similar expressions are found for the TM^z contribution, but are omitted here for the sake of brevity. Having now obtained the principal and reflected portions, the total Green's functions can be written in standing wave form, using Euler's identity. Each of the total Green's functions (*ee*-, *eh*-, *he*- and *hh*−type) are expanded component-wise and given explicitly in Appendix A for reference.

3. PHYSICAL INTERPRETATION AND POINTS OF INTEREST

In this section, we will discuss some interesting physical interpretations of the Green's functions and a primary application of these expressions. We begin with the reflected Green's function. The individual terms of the reflected Green's functions represent the fundamental set of possible paths of a wave emitted at a point $z = z'$ and observed at a point z. This is best illustrated by Figure 2. For example, the path

r_1 represents a upward propagating wave which reflects off of the lower boundary and corresponds to the first exponential term in (34). This path undergoes a phase shift of $z+z'$ while traveling from the source to the observer. Accordingly, the path r_2 represents an upward propagating wave which is reflected off both the upper and lower PEC plates and observed at the point z. This wave undergoes a phase shift of $(d-z')+(d)+z=2d+z-z'$ while traveling from the source to the observer and is represented by the second exponential term of (34). Paths r_3 and r_4 correspond to the third and fourth exponential terms of (34), respectively. Also, the principal contribution is shown, which is the direct path from the source to the observation point. Naturally, an infinite number of possibilities exist, which are accounted for by the poles in the denominator of the expressions. This is clearly the behavior one would expect inside a PPWG geometry. Additionally, one physical insight that is seen through the detailed application of the PEC boundary conditions in this direct method of solving Maxwell's equations is the lack of coupling between TE^z and TM^z waves at the PEC boundaries. Since the uniaxial constitutive parameter dyads do not contain any off-diagonal terms, we would not expect any coupling between TE^z and TM^z modes.

We can also glean appropriate physical insight from the total Green's functions. Let us consider the individual components of the eh- and hh-type Green's functions, given in (A3) and (A5). These represent the electric and magnetic fields maintained by a magnetic current. First, we note that $\tilde{G}^{\mathrm{TE}}_{eh,zx}$, $\tilde{G}^{\mathrm{TE}}_{eh,zy}$, $\tilde{G}^{\mathrm{TE}}_{eh,zz}=0$. This is, of course, the expected behavior, as $E_z=0$ is the very definition of a TE^z field. Furthermore, for the TM^z case, we know that $H_z=0$. From the expressions, we see $\tilde{G}^{\mathrm{TM}}_{eh,xz}$, $\tilde{G}^{\mathrm{TM}}_{eh,yz}$, $\tilde{G}^{\mathrm{TM}}_{eh,zz}=0$, which agrees with intuition, as any magnetic current with a component in the $\hat{\mathbf{z}}$ direction would also produce an magnetic field in that direction; therefore all z-directed magnetic sources must be zero. This fact also leads to $\tilde{G}^{\mathrm{TM}}_{hh,xz}$, $\tilde{G}^{\mathrm{TM}}_{hh,yz}$, $\tilde{G}^{\mathrm{TM}}_{hh,zx}$, $\tilde{G}^{\mathrm{TM}}_{hh,zy}$, $\tilde{G}^{\mathrm{TM}}_{hh,zz}=0$.

We can also assign physical meaning to the non-zero contributions by use of three illustrations. Let us first consider a $\hat{\mathbf{z}}$-directed magnetic current, J_{h_z} which maintains a non-zero magnetic field ($H_z\neq 0$). This would correspond to a TE^z wave and is shown in Figure 3(a). Clearly, this current produces a $\hat{\mathbf{z}}$-directed magnetic field, leading to $\tilde{G}^{\mathrm{TE}}_{hh,zz}\neq 0$. According to Maxwell's equations, we would have a rotational electric field consisting only of transverse ($\hat{\mathbf{x}}$ and $\hat{\mathbf{y}}$) components. Therefore, we see that $\tilde{G}^{\mathrm{TE}}_{eh,xz}$ and $\tilde{G}^{\mathrm{TE}}_{eh,yz}$ are non-zero, since $\hat{\mathbf{x}}$ and $\hat{\mathbf{y}}$ directed electric fields are produced from the $\hat{\mathbf{z}}$-directed magnetic current. Finally, we note from this case that a "secondary" magnetic field diverges from the center of this rotational electric field, leading to non-zero $\tilde{G}^{\mathrm{TE}}_{hh,xz}$, $\tilde{G}^{\mathrm{TE}}_{hh,yz}$ components. This field is shown in green in the Figure 3(a).

Now, consider a rotational magnetic current with only transverse components, $\vec{J}_{ht_r}$ (a TM^z wave). This situation is shown in Figure 3(b). The rotational current maintains a counter-rotating magnetic field, which gives rise to non-zero $\tilde{G}^{\mathrm{TM}}_{hh,xx}$, $\tilde{G}^{\mathrm{TM}}_{hh,xy}$, $\tilde{G}^{\mathrm{TM}}_{hh,yx}$, $\tilde{G}^{\mathrm{TM}}_{hh,yy}$ terms. Additionally, we see the electric field rotating around this transverse magnetic field, leading to all possible electric field components **except** $\tilde{G}^{\mathrm{TM}}_{eh,xz}$, $\tilde{G}^{\mathrm{TM}}_{eh,yz}$, and $\tilde{G}^{\mathrm{TM}}_{eh,zz}$, since a $\hat{\mathbf{z}}$-directed magnetic source is not allowed for a TM^z wave.

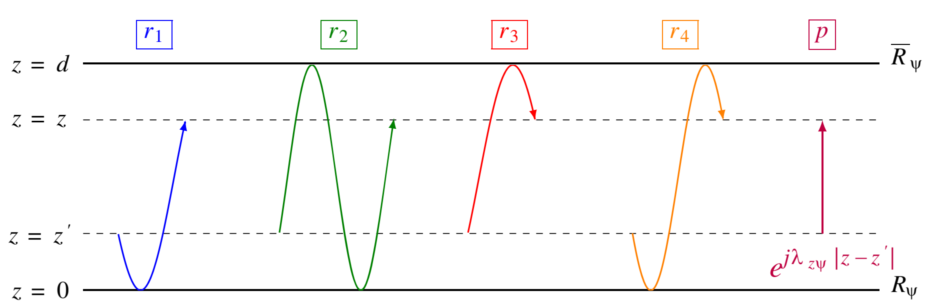

Figure 2. A visual representation of the terms given in (34). The terms represent waves that are reflected from the top and bottom of the parallel plate. The path r_1 represents the first term, path r_2 represents the second term, path r_3 represents the third term and the path r_4 represents the fourth. The principal solution is also shown on the far right.

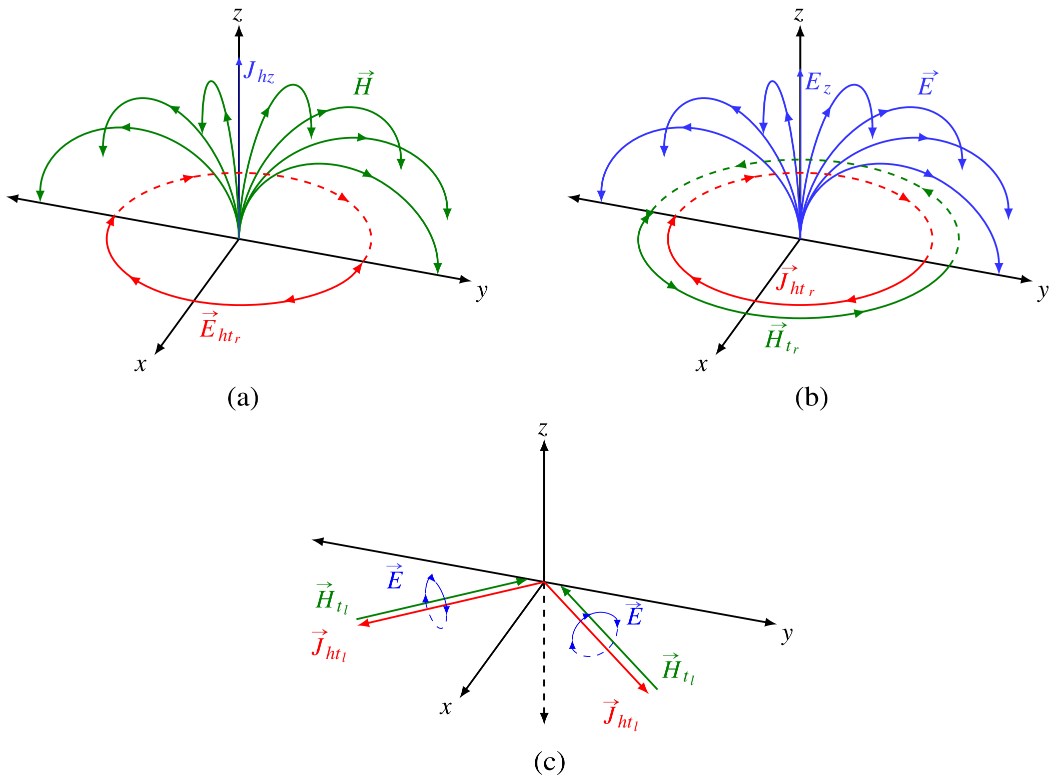

Figure 3. (a) The 3-D fields for a $\hat{\mathbf{z}}$-directed magnetic current, $\vec{J}_{h_z}$. (b) The 3-D fields for a transverse, rotating magnetic current $\vec{J}_{ht_r}$, viewed from the side. (c) Two notional vectors in a diverging lamellar current, shown in 3-D.

There is one further case to consider — that of a sheet of lamellar magnetic current in the transverse direction, $\vec{J}_{ht_l}$, maintaining a lamellar magnetic field, $\vec{H}_{ht_l}$. It is a bit more complicated to see that this is a TE^z case, but is shown graphically in Figure 3(c). Note that this sheet is actually comprised of an infinite density of vectors, but we have only shown two for clarity. It is clear that we have non-zero $\tilde{G}^{\mathrm{TE}}_{hh,xx}$, $\tilde{G}^{\mathrm{TE}}_{hh,xy}$, $\tilde{G}^{\mathrm{TE}}_{hh,yx}$, $\tilde{G}^{\mathrm{TE}}_{hh,yy}$ components. Also, in this case, we see the electric fields rotating around the lamellar magnetic field vectors, leading to non-zero $\tilde{G}^{\mathrm{TE}}_{eh,xx}$, $\tilde{G}^{\mathrm{TE}}_{eh,xy}$, $\tilde{G}^{\mathrm{TE}}_{eh,yx}$, $\tilde{G}^{\mathrm{TE}}_{eh,yy}$ components. Note that the $\hat{\mathbf{z}}$ components of adjacent rotating electric fields cancel one another out — leading to a net zero $\hat{\mathbf{z}}$ component; this allows us to see it as a TE^z field. A "secondary" magnetic field will diverge from the center of each rotating electric field, leading to non-zero $\tilde{G}^{\mathrm{TE}}_{hh,zx}$, $\tilde{G}^{\mathrm{TE}}_{hh,zy}$ components, similar to the "secondary" (green) magnetic field in Figure 3(a). From the preceding analysis, we see that each component of the Green's function is explicitly tied to the physical picture we would expect from a basic application of Maxwell's equations. A similar analysis holds for the terms associated with an electric current.

4. CONCLUSIONS

This paper has presented the detailed development of the total Green's functions, directly from Maxwell's equations, for a parallel plate waveguide (PPWG) filled with dielectric and magnetic uniaxial media. Due to the increased complexity introduced by allowing both dielectric and magnetic anisotropy, we see a significant increase in the amount of analysis required to obtain the desired expressions over [17], where only dielectric anisotropy was considered. This increase in work arises from two main areas: the manual algebraic inversion of a 3×3 matrix (since no simplifying identities were found) and the computation of the Green's function on a component-by-component basis. Although it may be possible to extend this direct solution of Maxwell's equations to more complex media (i.e., — gyrotropic), the substantial increase in work would likely make it an unattractive approach. These Green's functions are now available for use in a non-destructive evaluation configuration, such as the two-Flanged Waveguide Measurement Technique (tFWMT) given in [18, 19], for the extraction of the transverse and longitudinal permittivity and permeability of uniaxial media. This would represent a novel and exciting nondestructive characterization method for anisotropic media. Additionally, it paves the way for the nondestructive electromagnetic characterization of more general types of media (gyrotropic, chiral, etc.). Future work will concentrate on developing the tFWMT for use in characterizing uniaxial media.

APPENDIX A. EXPANDED TOTAL GREEN'S FUNCTIONS

Here, the total Green's functions are given component-wise. In order to present as compact a notation as possible, we define the following 8 terms (4 for $\lambda_{z\theta}$ and 4 for $\lambda_{z\psi}$):

$$\begin{aligned}
\Upsilon_1^\alpha &= \frac{\cos\left(\lambda_{z\alpha}\left[d-|z-z'|\right]\right)-\cos\left(\lambda_{z\alpha}\left[d-(z+z')\right]\right)}{\sin\left(\lambda_{z\alpha}d\right)} \\
\Upsilon_2^\alpha &= \frac{\cos\left(\lambda_{z\alpha}\left[d-|z-z'|\right]\right)+\cos\left(\lambda_{z\alpha}\left[d-(z+z')\right]\right)}{\sin\left(\lambda_{z\alpha}d\right)} \\
\Upsilon_3^\alpha &= \frac{\operatorname{sgn}(z-z')\sin\left(\lambda_{z\alpha}\left[d-|z-z'|\right]\right)-\sin\left(\lambda_{z\alpha}\left[d-(z+z')\right]\right)}{\sin\left(\lambda_{z\alpha}d\right)} \\
\Upsilon_4^\alpha &= \frac{\operatorname{sgn}(z-z')\sin\left(\lambda_{z\alpha}\left[d-|z-z'|\right]\right)+\sin\left(\lambda_{z\alpha}\left[d-(z+z')\right]\right)}{\sin\left(\lambda_{z\alpha}d\right)} \\
&\ldots \alpha = \theta, \psi
\end{aligned} \tag{A1}$$

A.1. *ee*-type Green's Function

$$\begin{aligned}
\tilde{\overleftrightarrow{G}}_{ee} &= \tilde{\overleftrightarrow{G}}_{ee}^{\mathrm{TE}} + \tilde{\overleftrightarrow{G}}_{ee}^{\mathrm{TM}} + \tilde{\overleftrightarrow{G}}_{ee}^{\mathrm{d}} \\
\tilde{\overleftrightarrow{G}}_{ee}^{\mathrm{TE}} &= \left(\frac{j\omega\mu_t}{2\lambda_{z\theta}\lambda_\rho^2}\right)\begin{bmatrix} \lambda_y^2 & -\lambda_x\lambda_y & 0 \\ -\lambda_x\lambda_y & \lambda_x^2 & 0 \\ 0 & 0 & 0 \end{bmatrix}\Upsilon_1^\theta \\
\tilde{\overleftrightarrow{G}}_{ee}^{\mathrm{TM}} &= \left(\frac{j}{2\omega\varepsilon_t\lambda_\rho^2}\right)\begin{bmatrix} \lambda_x^2\lambda_{z\psi}\Upsilon_1^\psi & \lambda_x\lambda_y\lambda_{z\psi}\Upsilon_1^\psi & j\frac{\varepsilon_t}{\varepsilon_z}\lambda_x\lambda_\rho^2\Upsilon_4^\psi \\ \lambda_x\lambda_y\lambda_{z\psi}\Upsilon_1^\psi & \lambda_y^2\lambda_{z\psi}\Upsilon_1^\psi & j\frac{\varepsilon_t}{\varepsilon_z}\lambda_y\lambda_\rho^2\Upsilon_4^\psi \\ j\frac{\varepsilon_t}{\varepsilon_z}\lambda_x\Upsilon_3^\psi & j\frac{\varepsilon_t}{\varepsilon_z}\lambda_y\lambda_\rho^2\Upsilon_3^\psi & \left(\frac{j}{\lambda_{z\psi}}\right)\left(\frac{\varepsilon_t\lambda_\rho^2}{\varepsilon_z}\right)^2\Upsilon_2^\psi \end{bmatrix} \\
\tilde{\overleftrightarrow{G}}_{ee}^{\mathrm{d}} &= -\frac{1}{j\omega\varepsilon_z}\delta(z-z')
\end{aligned} \tag{A2}$$

A.2. *eh*-type Green's Function

$$
\begin{aligned}
\tilde{\overleftrightarrow{G}}_{eh} &= \tilde{\overleftrightarrow{G}}_{eh}^{\text{TE}} + \tilde{\overleftrightarrow{G}}_{eh}^{\text{TM}} \\
\tilde{\overleftrightarrow{G}}_{eh}^{\text{TE}} &= \left(\frac{1}{2\lambda_\rho^2}\right)\begin{bmatrix} -\lambda_x\lambda_y\Upsilon_4^\theta & -\lambda_y^2\Upsilon_4^\theta & \dfrac{j\mu_t\lambda_y\lambda_\rho^2}{\mu_z\lambda_{z\theta}}\Upsilon_1^\theta \\ \lambda_x^2\Upsilon_4^\theta & \lambda_x\lambda_y\Upsilon_4^\theta & -\dfrac{j\mu_t\lambda_x\lambda_\rho^2}{\mu_z\lambda_{z\theta}}\Upsilon_1^\theta \\ 0 & 0 & 0 \end{bmatrix} \\
\tilde{\overleftrightarrow{G}}_{eh}^{\text{TM}} &= \left(\frac{1}{2\lambda_\rho^2}\right)\begin{bmatrix} \lambda_x\lambda_y\Upsilon_4^\psi & -\lambda_x^2\Upsilon_4^\psi & 0 \\ \lambda_y^2\Upsilon_4^\psi & -\lambda_x\lambda_y\Upsilon_4^\psi & 0 \\ -\dfrac{j\varepsilon_t\lambda_y\lambda_\rho^2}{\varepsilon_z\lambda_{z\psi}}\Upsilon_2^\psi & \dfrac{j\varepsilon_t\lambda_x\lambda_\rho^2}{\varepsilon_z\lambda_{z\psi}}\Upsilon_2^\psi & 0 \end{bmatrix}
\end{aligned}
\tag{A3}
$$

A.3. *he*-type Green's Function

$$
\begin{aligned}
\tilde{\overleftrightarrow{G}}he &= \tilde{\overleftrightarrow{G}}_{he}^{\text{TE}} + \tilde{\overleftrightarrow{G}}_{he}^{\text{TM}} \\
\tilde{\overleftrightarrow{G}}_{he}^{\text{TE}} &= \left(\frac{1}{2\lambda_\rho^2}\right)\begin{bmatrix} -\lambda_x\lambda_y\Upsilon_3^\theta & \lambda_x^2\Upsilon_3^\theta & 0 \\ -\lambda_y^2\Upsilon_3^\theta & \lambda_x\lambda_y\Upsilon_3^\theta & 0 \\ \dfrac{j\mu_t\lambda_y\lambda_\rho^2}{\mu_z\lambda_{z\theta}}\Upsilon_1^\theta & -\dfrac{j\mu_t\lambda_x\lambda_\rho^2}{\mu_z\lambda_{z\theta}}\Upsilon_1^\theta & 0 \end{bmatrix} \\
\tilde{\overleftrightarrow{G}}_{he}^{\text{TM}} &= \left(\frac{1}{2\lambda_\rho^2}\right)\begin{bmatrix} \lambda_x\lambda_y\Upsilon_3^\psi & \lambda_y^2\Upsilon_3^\psi & -\dfrac{j\varepsilon_t\lambda_y\lambda_\rho^2}{\varepsilon_z\lambda_{z\psi}}\Upsilon_2^\psi \\ -\lambda_x^2\Upsilon_4^\psi & -\lambda_x\lambda_y\Upsilon_3^\psi & \dfrac{j\mu_t\lambda_x\lambda_\rho^2}{\mu_z\lambda_{z\psi}}\Upsilon_2^\psi \\ 0 & 0 & 0 \end{bmatrix}
\end{aligned}
\tag{A4}
$$

A.4. *hh*-type Green's Function

$$
\begin{aligned}
\tilde{\overleftrightarrow{G}}_{hh} &= \tilde{\overleftrightarrow{G}}_{hh}^{\text{TE}} + \tilde{\overleftrightarrow{G}}_{hh}^{\text{TM}} + \tilde{\overleftrightarrow{G}}_{hh}^{\text{d}} \\
\tilde{\overleftrightarrow{G}}_{hh}^{\text{TE}} &= \left(\frac{j}{2\omega\mu_t\lambda_\rho^2}\right)\begin{bmatrix} \lambda_x^2\lambda_{z\theta}\Upsilon_2^\theta & \lambda_x\lambda_y\lambda_{z\psi}\Upsilon_2^\theta & j\dfrac{\mu_t}{\mu_z}\lambda_x\lambda_\rho^2\Upsilon_3^\theta \\ \lambda_x\lambda_y\lambda_{z\theta}\Upsilon_2^\theta & \lambda_y^2\lambda_{z\theta}\Upsilon_2^\theta & j\dfrac{\mu_t}{\mu_z}\lambda_y\lambda_\rho^2\Upsilon_3^\theta \\ j\dfrac{\mu_t}{\mu_z}\lambda_x\Upsilon_4^\theta & j\dfrac{\mu_t}{\mu_z}\lambda_y\lambda_\rho^2\Upsilon_4^\theta & \left(\dfrac{j}{\lambda_{z\psi}}\right)\left(\dfrac{\mu_t\lambda_\rho^2}{\mu_z}\right)^2\Upsilon_1^\theta \end{bmatrix} \\
\tilde{\overleftrightarrow{G}}_{hh}^{\text{TM}} &= \left(\frac{j\omega\varepsilon_t}{2\lambda_{z\psi}\lambda_\rho^2}\right)\begin{bmatrix} \lambda_y^2 & -\lambda_x\lambda_y & 0 \\ -\lambda_x\lambda_y & \lambda_x^2 & 0 \\ 0 & 0 & 0 \end{bmatrix}\Upsilon_2^\psi \\
\tilde{\overleftrightarrow{G}}_{hh}^{\text{d}} &= -\frac{1}{j\omega\mu_z}\delta(z-z')
\end{aligned}
\tag{A5}
$$

Note, the total spatial-domain fields may be found by dotting the total dyadic Green's function terms in (A2)–(A5) by the appropriate current, followed by Fourier inversion via (3), the details of which are omitted for the sake of brevity.

REFERENCES

1. Ali, S. M., T. M. Habashy, and J. A. Kong, "Spectral-domain Green's function in layered chiral media," *JOSA A*, Vol. 9, No. 3, 413–423, 1992.
2. Bagby, J. S. and D. P. Nyquist, "Dyadic Green's functions for integrated electronic and optical circuits," *IEEE Transactions on Microwave Theory and Techniques*, Vol. 35, No. 2, 207–210, 1987.
3. Balanis, C. A., *Advanced Engineering Electromagnetics*, Vol. 205, Wiley, New York, 1989.
4. Ball, J. A. R. and P. J. Khan, "Source region electric field derivation by a dyadic Green's function approach," *IEE Proceedings H — Microwaves, Optics and Antennas*, Vol. 127, No. 5, 301–304, 1980.
5. Chang, C. W., K. M. Chen, and J. Qian, "Nondestructive measurements of complex tensor permittivity of anisotropic materials using a waveguide probe system," *IEEE Transactions on Microwave Theory and Techniques*, Vol. 44, No. 7, 1081–1090, 1996.
6. Chang, C. W., K. M. Chen, and J. Qian, "Nondestructive determination of electromagnetic parameters of dielectric materials at x-band frequencies using a waveguide probe system," *IEEE Transactions on Instrumentation and Measurement*, Vol. 46, No. 5, 1084–1092, 1997.
7. Chen, H. C., *Theory of Electromagnetic Waves: A Coordinate-free Approach*, McGraw-Hill Book Company, 1983.
8. Chen, K. M., "A simple physical picture of tensor Green's function in source region," *Proceedings of the IEEE*, Vol. 65, No. 8, 1202–1204, 1977.
9. Chew, W. C., "Some observations on the spatial and eigenfunction representations of dyadic Green's functions," *IEEE Transactions on Antennas and Propagation*, Vol. 37, No. 10, 1322–1327, 1989.
10. Chew, W. C., *Waves and Fields in Inhomogeneous Media*, Van Nostrand Reinhold, 1990.
11. De Visschere, P., *Electromagnetic Source Transformations and Scalarization in Stratified Gyrotropic Media*, ArXiv e-prints, June 2009.
12. Dester, G. D., E. J. Rothwell, and M. J. Havrilla, "An extrapolation method for improving waveguide probe material characterization accuracy," *IEEE Microwave and Wireless Components Letters*, Vol. 20, No. 5, 298–300, 2010.
13. Fikioris, J. G., "Electromagnetic field inside a current-carrying region," *Journal of Mathematical Physics*, Vol. 6, 1617, 1965.
14. Georgieva, N. K. and W. S. Weiglhofer, "Electromagnetic vector potentials and the scalarization of sources in a nonhomogeneous medium," *Phys. Rev. E*, Vol. 66, 046614, Oct. 2002.
15. Harrington, R. F., *Time-harmonic Electromagnetic Fields*, McGraw-Hill Electrical and Electronic Engineering Series, McGraw-Hill, 1961.
16. Havrilla, M., "Electric and magnetic field dyadic Green's functions and depolarizing dyad for a magnetic current immersed in a uniaxial dielectric-filled parallel plate waveguide," *2011 XXXth URSI General Assembly and Scientific Symposium*, 1–4, 2011.
17. Havrilla, M. J., "Scalar potential depolarizing dyad artifact for a uniaxial medium," *Progress In Electromagnetics Research*, Vol. 134, 151–168, 2013.
18. Hyde IV, M. W. and M. J. Havrilla, "A non-destructive technique for determining complex permittivity and permeability of magnetic sheet materials using two flanged rectangular waveguides," *Progress In Electromagnetics Research*, Vol. 79, 367–386, 2008.
19. Hyde, M. W., M. J. Havrilla, and A. E. Bogle, "A novel and simple technique for measuring low-loss materials using the two flanged waveguides measurement geometry," *Measurement Science and Technology*, Vol. 22, No. 8, 085704, 2011.
20. Jakoby, B. and F. Olyslager, "Singularity in green dyadics for uniaxial bianisotropic media," *Electronics Letters*, Vol. 31, No. 10, 779–781, 1995.
21. Lindell, I. V. and F. Olyslager, "Potentials in bi-anisotropic media," *Journal of Electromagnetic Waves and Applications*, Vol. 15, No. 1, 3–18, 2001.
22. Lindell, I. V., A. H. Sihvola, and S. Tretyakov, *Electromagnetic Waves in Chiral and Bi-isotropic Media*, Artech House, Inc, Norwood, MA, 1994.

23. Mackay, T. G. and A. Lakhtakia, *Electromagnetic Anisotropy and Bianisotropy: A Field Guide*, World Scientific Publishing Company Incorporated, 2010.
24. Niu, M., Y. Su, J. Yan, C. Fu, and D. Xu, "An improved open-ended waveguide measurement technique on parameters ε_γ and μ_γ of high-loss materials," *IEEE Transactions on Instrumentation and Measurement*, Vol. 47, No. 2, 476–481, ID: 1, 1998.
25. Przeziecki, S. and R. A. Hurd, "A note on scalar hertz potentials for gyrotropic media," *Applied Physics*, Vol. 20, No. 4, 313 –317, 1979.
26. Seal, M. D., M. W. Hyde IV, and M. J. Havrilla, "Nondestructive complex permittivity and permeability extraction using a two-layer dual-waveguide probe measurement geometry," *Progress In Electromagnetics Research*, Vol. 123, 123–142, 2012.
27. Stratton, J. A., *Electromagnetic Theory*, IEEE Press Series on Electromagnetic Wave Theory, Wiley, 2007.
28. Van Bladel, J., "Some remarks on Green's dyadic for infinite space," *IRE Transactions on Antennas and Propagation*, Vol. 9, No. 6, 563–566, 1961.
29. Viola, M. S. and D. P. Nyquist, "An observation on the Sommerfeld-integral representation of the electric dyadic Green's function for layered media," *IEEE Transactions on Microwave Theory and Techniques*, Vol. 36, No. 8, 1289–1292, 1988.
30. Weiglhofer, W. S., "Scalarisation of Maxwell's equations in general inhomogeneous bianisotropic media," *IEE Proceedings H — Microwaves, Antennas and Propagation*, Vol. 134, No. 4, 357–360, August 1987.
31. Weiglhofer, W. S., "Frequency-dependent dyadic green functions for bianisotropic media," *Advanced Electromagnetism: Foundations, Theory, Applications*, 376–389, 1995.
32. Weiglhofer, W. S., "Electromagnetic field in the source region: A review," *Electromagnetics*, Vol. 19, No. 6, 563–577, 1999.
33. Weiglhofer, W. S., "Hertz potentials in complex medium electromagnetics," Technical report, DTIC Document, 2000.
34. Weiglhofer, W. S., *Scalar Hertz Potentials for Linear Bianisotropic Mediums*, John Wiley, 2000.
35. Weiglhofer, W. S., "Scalar hertz potentials for nonhomogeneous uniaxial dielectric-magnetic mediums," *International Journal of Applied Electromagnetics and Mechanics*, Vol. 11, No. 3, 131–140, 2000.
36. Weiglhofer, W. S and S. O. Hansen, "Faraday chiral media revisited. I. Fields and sources," *IEEE Transactions on Antennas and Propagation*, Vol. 47, No. 5, 807–814, May 1999.
37. Weiglhofer, W. S. and A. Lakhtakia, "Introduction to complex mediums for optics and electromagnetics," *Society of Photo Optical*, Vol. 123, 2003.
38. Yaghjian, A. D., "Electric dyadic green's functions in the source region," *Proceedings of the IEEE*, Vol. 68, No. 2, 248–263, 1980.